Effect of enantiomeric excess on the phase behavior of antiferroelectric liquid crystals

LiDong Pan, B. K. McCoy, Shun Wang, Z. Q. Liu, S. T. Wang, R. Pindak, and C. C. Huang

Phys. Rev. E **83**, 060701 — Published 14 June 2011

DOI: 10.1103/PhysRevE.83.060701

Effect of Enantiomeric Excess on the Phase Behavior of Antiferroelelctric Liquid Crystal

LiDong Pan,[1] B. K. McCoy,[1,2] Shun Wang,[1] Z. Q. Liu,[1,3] S. T. Wang,[4,5] R. Pindak,[6] and C. C. Huang[1]

[1]*School of Physics and Astronomy, University of Minnesota, Minneapolis, Minnesota 55455*
[2]*Department of Mathematics and Physics, Azusa Pacific University, Azusa, California 91702*
[3]*Department of Physics, Astronomy, and Engineering Science, St. Cloud State University, St. Cloud, Minnesota 56301*
[4]*NSLS, Brookhaven National Laboratory, Upton, New York 11973*
[5]*Laboratory of Atomic and Solid State Physics, Cornell University, Ithaca, NY 14853*
[6]*Photon Sciences Directorate, Brookhaven National Laboratory, Upton, New York 11973*

Null transmission ellipsometry and resonant x-ray diffraction were employed to study the effect of enantiomeric excess (EE) on the phase behavior of antiferroelectric liquid crystal 10OTBBB1M7. Phase sequence, layer spacing as well as pitch of the helical structures of the smectic-C^*_α and smectic-C^* phase were studied as a function of temperature and EE. Upon reducing EE, a liquid-gas type critical point of the smectic-C^*_α - smectic-C^* transition was observed, as well as the disappearance of the smectic-C^*_{d4} and the smectic-C^*_{d3} phases. Results were analysed in a mean field model.

PACS numbers: 61.30.Hn, 64.70.Md, 77.84.Nh

The discovery of new phases and the elucidating of their structures have always been important topics in physics. However, the identification of the interactions stabilizing those structures or the forces driving the phase transitions among them can be a very challenging task. Antiferroelectric liquid crystal (AFLC) materials and the smectic-C* (SmC^*, in which molecules arranged in layers and are titled away from the layer normal) variant phases special to those materials were discovered about two decades ago [1]. Although the structures of these phases have been established by resonant x-ray diffraction (RXRD) [2] and various optical methods [3–5], the understanding of the forces responsible for those structures and the transitions between them is still limited.

The structural model established for the SmC^* variant phases is called the "distorted clock model". Different phases are characterized with different azimuthal arrangements of tilt directions among layers. Within each layer, the tilt directions are uniform if no defects are present. The smectic-C^*_α (SmC^*_α) and SmC^* phase are featured with a helical structure with pitch on the order of nanometers and micrometers, respectively. The smectic-C^*_{d4} (SmC^*_{d4}) and smectic-C^*_{d3} (SmC^*_{d3}) phase have 4-layer and 3-layer unit cell with structures discussed in detail in Ref. 3. The recently discovered smectic-C^*_{d6} phase has a 6-layer unit cell [6].

One reason for the limited understanding for the SmC^* variant phases is the many competing interactions involved [7], thus resulting in a very complicated phase diagram. The phase diagram of AFLC materials is multi-dimensional, with temperature (T), enantiomeric excess (EE, also called optical purity), external electric field, surface anchoring strength, concentration in a mixture system all being tunable parameters that can affect the behavior of the sample. Thus to gain a better understanding of the physics of AFLC materials, it is beneficial to study the effects of those parameters as selectively and quantitatively as possible.

In this paper we report our experimental results on the effect of EE on the behavior of one AFLC material. Phase sequences, transition temperatures as well as layer spacing and pitch data were obtained as a function of T and EE. Although phase sequences and switching behavior have been studied as a function of EE [9–11], no previous study has reported its effect on the temperature variation of the tilt angle or the pitch of the AFLC material. Thus our results will provide new information for

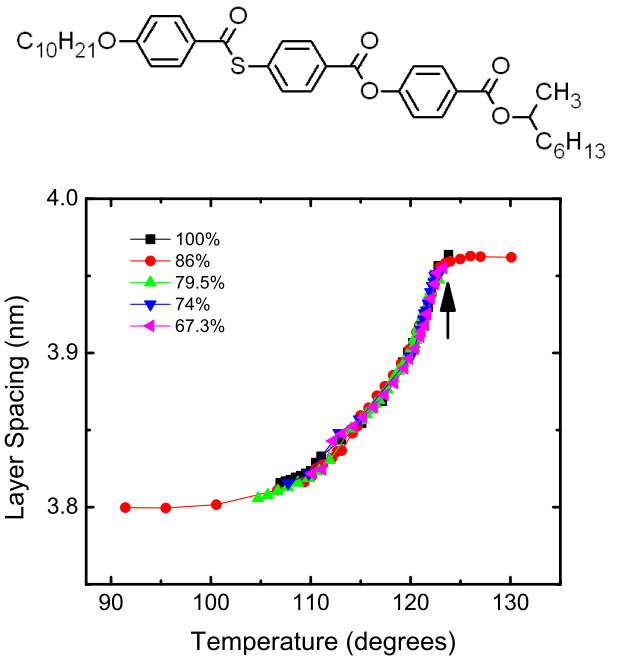

FIG. 1: (Color online) Layer spacing measured from RXRD as a function of T for different mixtures. The arrow marks the SmA-SmC^*_α transition temperature. On the top is the chemical structure of 10OTBBB1M7 (C10). [8]

understanding the behavior of AFLC, as well as new insights on the driving forces for the SmC^* variant phases.

The material used for this study is AFLC compound C10 (R-, optically pure) and its enatiomeric mixtures [12]. The molecular structure of C10 is shown at the top of Fig. 1. Enantiomeric mixtures were prepared by mixing R-C10 with racemic-C10. Enantiomeric excess (EE) is defined by the weight percentage of R-C10 in the mixtures. Mixtures with EE equals to 67.3%, 74%, 79.5%, 86% and 100% (R-) were prepared and studied for this project.

The RXRD experiments were carried out at beam line X19A in National Synchrotron Light Source (NSLS), Brookhaven National Laboratory (BNL). Since different SmC^* variant phases have different unit cell sizes, measurement of this quantity is essential for the study of AFLC materials. So far, RXRD remains the most powerful and most straight forward method for this task. At the resonant energy of the sulphur atom in C10 molecule, satellite peaks appear in the q-scan in addition to the Bragg peaks due to the layered structures of the smectic phases. Size of the unit cell can be determined from the relative positions of the satellite peaks and the Bragg peak. For simple helical structures like the SmC^*_α and the SmC^* phase, the size of the unit cell equals to the pitch of the helix. Details of the RXRD experiments have been reported elsewhere [13].

Figure 1 shows the layer spacing d as a function of T from mixtures with various values of EE. As shown in the figure, data from different samples collapse quite well onto one single curve over the temperature range studied. This indicates that the behavior of the tilt angle is not affected by the change in EE for the mixtures studied.

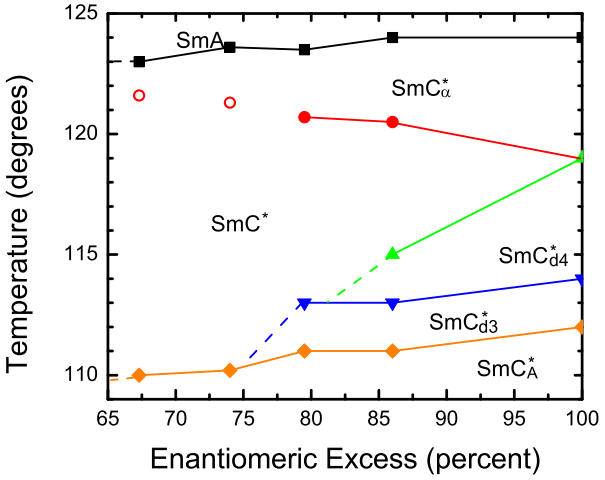

FIG. 2: (Color online) Phase diagram of C10 mixtures as a function of T and EE. Transition temperatures were marked with symbols and phase boundaries with lines. The SmC^*_α - SmC^* transition in the 67.3% and 74% EE mixtures were marked with open symbols to represent the supercritical nature of the transition in this region.

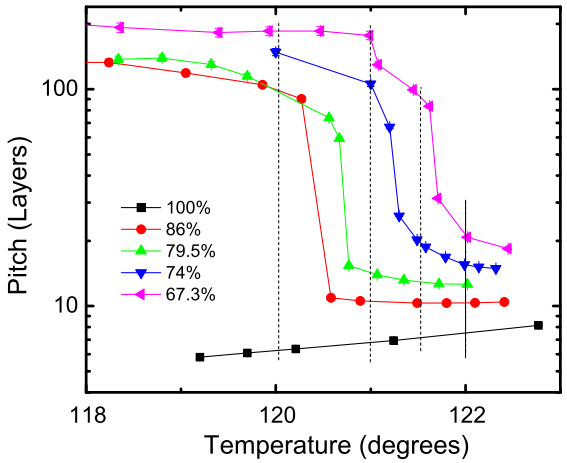

FIG. 3: (Color online) Pitch of the SmC^*_α and the SmC^* structures near the transition as a function of temperature and EE. Log scale is used for the vertical axis in order for the pitch behavior of the SmC^*_α phase to be visible. Vertical dashed lines mark T = 122°C, 121.5°C, 121°C, and 120°C from where data in Fig. 4 (a) were taken.

Thus the different behaviors of SmC^* variant phases in different samples as shown in Fig. 2 are driven by factors other than the tilt angle evolution. This situation is very different from the results reported in Ref. 14 and 15, where pronounced changes in layer spacing were observed in the phase diagram.

Figure 2 shows the phase diagram as a function of T and EE obtained from our in-house Null Transmission Ellipsometry (NTE) and confirmed with RXRD experiments. In the phase diagram, symbols mark the transition temperatures while lines represent phase boundaries (Dashed lines were used when a phase boundary ends between data points).

Figure 2 shows the following three main features: a) the tilt transition temperature T_{AC} is only weakly affected by the change of EE (from NTE results, about 1°C change in T_{AC} is observed among the different mixtures studied, while from the RXRD data, the change observed from layer spacing data in Fig. 1 seems to be smaller); b) As EE decreases, the SmC^*_{d4} phase disappears first, followed by SmC^*_{d3}, while the SmC^* window increases; c) A SmC^*_α-SmC^* critical point is observed in the phase diagram. While the first two behaviors have been reported [9, 10], it is the first time for the observation of a SmC^*_α-SmC^* critical point with EE and T being the two system parameters. In the following part of this paper, we will be focusing on the pitch evolution of SmC^*_α and SmC^* phases.

Shown in Fig. 3 are the pitch evolution P(T) measured from samples with different EE. As we can see from the data, mixtures with a high EE value (86% and 79.5%) exhibit a discontinuous SmC^*_α-SmC^* transition, where a sudden jump of pitch is observed upon cooling; while

mixtures with lower EE value (74% and 67.3%) exhibit continuous evolution of the pitch as we change temperature, which indicates that those two mixtures are in the supercritical region. Since the SmC^*_α-SmC^* transition is a transition between short pitched structures and long pitched structures, there's no fundamental symmetry change across the transition. Thus we expect to find a liquid-gas type critical point in the phase diagram. This critical point can be accessed by studying the pitch behavior P(T) as a function of EE, with the critical mixture having an EE value between 74% and 79.5%.

As discussed, the critical mixture is located between 74% and 79.5% EE. Thus for mixtures with EE value below the critical value EE_C, one cannot distinguish the SmC^*_α from the SmC^* phases. For this critical point, EE and T are the ordering fields, with EE corresponding to temperature and T corresponding to pressure in the liquid-gas transition [16]. Thus the change of pitch at the transition ΔP is a natural choice of order parameter for this transition, with $\Delta P \propto (EE_C - EE)^\beta$. For mixtures in the supercritical region, the derivative dP/dT would show a cusp at the crossover temperature from the low-pitched SmC^*_α like side to the high-pitched SmC^* like side. The value of dP/dT at the cusp should be a function of reduced EE as well: $dP/dT_{cross} \propto (EE - EE_C)^{-\gamma}$. On the critical mixture with EE = EE_C, the evolution of the order parameter is determined by the ordering field T, with $P - P_C \propto (T - T_C)^{1/\delta}$. β, γ, and δ are all critical exponents for this transition. Since δ is expected to have the same value above and below T_C, when plotted in log-log scale, |P-P_C| as a function of |T-T_C| is expected to be parallel for T > T_C and T < T_C [12]. This rule of phase transition should be followed when choosing the order parameter and determining the position of the critical point [17].

To the best of our knowledge, there are at least three different routes that allow one to explore the SmC^*_α-SmC^* critical point. One is the method we report in this paper, by reducing EE of C10. The second one is by studying mixtures of compound showing first order and supercritical SmC^*_α-SmC^* transition [18]. Here we argue the first method is superior, because it minimized the complications brought in through the different SmA-SmC^*_α transition temperatures in the mixtures with other compounds. Thus for the second method, it is not possible to perform scaling analysis on the data. Although for our experiments we do not have high enough data density or mixtures with different EE values to perform a scaling analysis, it is in principle doable. The third possible method to study the SmC^*_α-SmC^* critical behavior would be to perform pitch measurement on a sample with a weakly first order SmC^*_α - SmC^* transition. By studying the pitch behavior as a function of temperature and external transverse field (which has been shown to unwind the helix of the SmC^*_α, and SmC^* structures), a complete picture of the SmC^*_α - SmC^* critical point could be obtained.

To gain further understanding of the experimental results, we employed a simple model for the helical structures. The relevant free energy is:

$$F = J_1 \sum_{i=1}^{n} \boldsymbol{\xi_i} \cdot \boldsymbol{\xi_{i+1}} + J_2 \sum_{i=1}^{n} \boldsymbol{\xi_i} \cdot \boldsymbol{\xi_{i+2}} \qquad (1)$$

Here J_1 is the nearest neighbour (NN) interlayer interaction. J_1 can be either ferroelectric or antiferroelectric. J_2 is the antiferroelectric next nearest neighbour (NNN) interlayer interaction. ξ_i is a unit vector describing the tilt direction of the ith layer. The frustration between the NN and the NNN interlayer interaction will produce a helical structure, with an angle ϕ between neighbouring layers given by:

$$\cos(\phi) = -J_1/4J_2 \qquad (2)$$

with -1 $\leq \frac{J_1}{4J_2} \leq$ 1.

Several previous studies have shown that the $J_1 - J_2$ model is too simple to describe the SmC^*_α - SmC^* transition [19, 20]; and for samples showing a first order SmC^*_α-SmC^* transition (79.5% and 86%), it requires a discontinuity in the temperature evolution of the J_2/J_1 value, which is quite unphysical. However, at this moment, there's no satisfactory theory available for the SmC^*_α-SmC^* transition. Thus, the $J_1 - J_2$ model can still give useful information about the behaviors observed with different EE values.

From Eq. 2 and Fig. 3, we obtained Fig. 4(a), showing the value of J_2/J_1 calculated from P(T) data obtained from mixtures with different EE values at T = 120°C, 121°C, 121.5°C, and 122°C. From the figure, we can see that not only does the value of $|J_2/J_1|$ decrease with decreasing EE value, the temperature derivative of $|J_2/J_1|$ also changes sign upon reducing EE. In the optically pure sample, no SmC^* phase was observed and the pitch in SmC^*_α phase shows a monotonic decrease upon cooling. This gives a $|J_2/J_1|$ that increases monotonically with decreasing temperature. However, from samples with low EE value (67.3% and 74%), there's a monotonic decrease of $|J_2/J_1|$ value upon cooling. These different behaviors are illustrated in Fig. 4(b) with two arrows.

Figure 4(b) shows the phase diagram of the $J_1 - J_2$ model. In this model, there are three phases, SmC, SmC_A and the helical phase (corresponding to both SmC^*_α and SmC^*). (Since no chiral interaction is considered in this model, the resulting structures are not chiral.) Arrow 1(2) represents the behavior of the optically pure sample (67.3% and 74% EE samples) upon cooling. As shown in this figure, change of EE in AFLC not only changes the position of the sample in the phase diagram, it can also change the direction of the sample's temperature evolution completely.

From Fig. 4(a), the value of $|J_2/J_1|$ shows a monotonic decrease with decreasing EE. Although due to the limitation of the $J_1 - J_2$ model, there is a lower bound of 0.25 for the value of $|J_2/J_1|$ calculated from the data, this observation still bears important information. First, with decreased EE, the pitch of the helical structure increases.

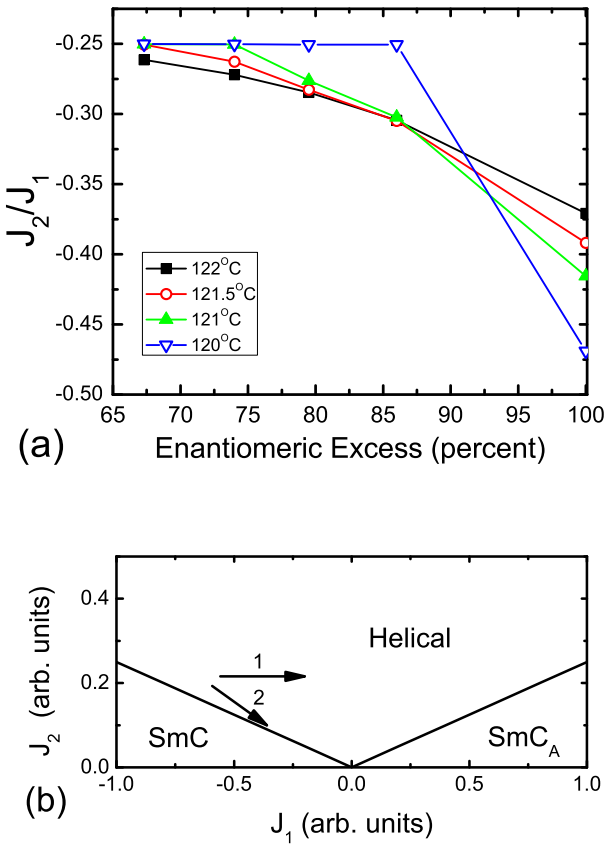

FIG. 4: (Color online) (a) J_2/J_1 as a function of EE calculated from Eq. 2 and pitch data obtained at T = 120°C, 121°C, 121.5°C, and 122°C. (b) Phase diagram of the $J_1 - J_2$ model, arrows 1 and 2 illustrate the behavior upon cooling of the optically pure sample and samples with low EE value. The direction of the arrows points to lower temperature.

This indicates a reduced twisting power of the liquid crystal sample and is consistent with the understanding that the twisting power of liquid crystal materials is related to the net sample chirality/optical purity. Second, a reduction of $|J_2/J_1|$ value suggests a reduced level of frustration in mixtures with lower EE values. Although at this moment there is no satisfying theory for the formation of the SmC^* variant phases in AFLC, it is generally agreed that frustration between different interactions is responsible for the intermediate phases and structures observed. A decreased level of frustration would thus results in lowered stability of those phases, as observed from Fig. 2. Although the model used is still rough, our results give a first quantitative account for the phase behavior of AFLC as a function of EE.

To summarize, we studied the effect of enantiomeric excess on the behavior of SmC^* variant phases in compound C10. We found that with decreasing EE value, 1) the SmC^* variant phases give way to SmC^*, 2) the pitch of the helical structure increases, 3) a liquid-gas type critical point of the SmC^*_α - SmC^* transition was observed. Analysing the data with a simple $J_1 - J_2$ model, we found that those observations indicate reduced twisting power and decreased level of frustration when EE is lowered.

This research was supported in part by the National Science Foundation, Solid State Chemistry Program, under Grant No. DMR-0605760. Use of the NSLS, BNL, was supported by the U.S. Department of Energy, Office of Science, Office of Basic Energy Sciences, under Contract No. DE-AC02-98CH10886. L. D. P. acknowledges the financial support from University of Minnesota Graduate School under DDF program in the final stage of this project. The authors would like to thank Dr. P. Barois for lending us the oven for the x-ray experiments, and Dr. H. T. Nguyen for supplying the high quality C10 compounds.

[1] T. Niori *et al.*, *J. Mater. Chem.* **6**, 1231 (1996).
[2] P. Mach *et al.*, *Phys. Rev. Lett.* **81**, 1015 (1998).
[3] P. M. Johnson *et al.*, *Phys. Rev. Lett.* **84**, 4870 (2000).
[4] D. Konovalov *et al.*, *Phys. Rev. E* **64**, 010704(R) (2001).
[5] M. Škarabot *et al.*, *Phys. Rev. E* **58**, 575 (1998).
[6] S. Wang *et al.*, *Phys. Rev. Lett.* **104**, 027801 (2010).
[7] R. Bruinsma and J. Prost, *J. Phys. II* **4**, 01209 (1994).
[8] Data for the mixture with 86% EE has been shifted down by 0.02nm, the difference from other mixtures are probably due to difference in the calibration of the set up.
[9] A. Cady *et al.*, *Phys. Rev. E* **66**, 061704 (2002).
[10] E. Gorecka *et al.*, *Phys. Rev. E* **65**, 061703 (2002).
[11] M. R. Dodge and C. Rosenblatt, *Phys. Rev. E* **62**, 6891 (2000).
[12] The phase sequence reported for R-C10 is: isotropic (153 °C) SmA (124 °C) SmC^*_α (120 °C) SmC^* (119 °C) SmC^*_{d4} (114 °C) SmC^*_{d3} (112 °C) SmC^*_A (110 °C) crystal. However, no SmC^* phase was observed in R-C10 from RXRD or NTE.
[13] P. Mach *et al.*, *Phys. Rev. E* **60**, 6793 (1999).
[14] S. Jaradat *et al.*, *J. Mater. Chem.* **16**, 3753 (2006).
[15] J. Kirchhoff and L. S. Hirst, *Phys. Rev. E* **76**, 051704 (2007).
[16] M. E. Fisher, in Lecture Notes in Physics, edited by F. J. W. Hahne (Springer-Verlag, Berlin, 1983) Vol. 186, Chapter 1.
[17] For the choice of order parameter and determination of the critical point, authors of Ref. 14 argued that on the critical isotherm, the behavior of the order parameter should be the symmetric about critical point, i.e., the ratio of the critical amplitude be one. This puts an additional constraint to the data analysis that is not necessary. Under this constraint, square root of pitch was chosen as the quantity related to the order parameter in Ref. 14.
[18] Z. Q. Liu *et al.*, *Phys. Rev. E* **74**, 030702 (2006).
[19] A. Cady *et al.*, *Phys. Rev. E* **65**, 030701 (2002).
[20] V. P. Panov *et al.*, *Phys. Rev. E* **74**, 011701 (2006).